PCCP

RSC Publishing

PAPER

View Article Online
View Journal | View Issue

Cite this: *Phys. Chem. Chem. Phys.*, 2013, **15**, 17647

Intraparticle donor–acceptor dyads prepared using conjugated metal–ligand linkages†

Bruce D. Phebus,[a] Yi Yuan,[b] Yang Song,[a] Peiguang Hu,[a] Yashar Abdollahian,[a] Qing-Xiao Tong*[b] and Shaowei Chen*[a]

Received 21st June 2013,
Accepted 13th August 2013

DOI: 10.1039/c3cp52584h

www.rsc.org/pccp

Ruthenium nanoparticles were stabilized by the self-assembly of 1-decyne forming ruthenium–vinylidene interfacial bonds and further functionalized by metathesis reactions with 4-ethynyl-*N*,*N*-diphenylaniline (EDPA) and 9-vinylanthracene (VAN). Photoluminescence studies of the resulting bifunctionalized Ru(EDPA/VAN) nanoparticles showed that as both ligands were bound onto the nanoparticle surface, effective mixing of the π electrons occurred leading to the appearance of excitation and emission profiles that were completely different from those of ruthenium nanoparticles functionalized with only EDPA or VAN. Furthermore, in photoelectrochemical studies, the EDPA moieties exhibited a pair of well-defined voltammetric peaks in the dark, which were ascribed to the redox reaction involving the formation of cationic radicals; however under UV photoirradiation the voltammetric features diminished markedly. These results strongly suggest that the particle-bound EDPA and VAN moieties behaved analogously to those of conventional molecular dyads based on the same electron-donating and -accepting units, where the intraparticle charge transfer was facilitated by the conjugated metal–ligand interfacial bonds.

Introduction

Conventional molecular dyads refer to a class of functional molecular complexes that consist of an electron-donating moiety and an electron-accepting counterpart linked by a chemical bridge. Upon photoirradiation, effective intramolecular electron and/or energy transfer may occur, leading to the emergence of unprecedented optical and electronic properties that may be exploited for diverse applications in, for instance, molecular electronics, electroluminescence, and organic photovoltaics.[1–3] Of these, anthracene derivatives have been used rather extensively as effective electron acceptors with apparent emission in the blue region, whereas common electron donors include derivatives of triphenylamine, carbazole, and phenothiazine that are known to facilitate hole transport (high hole mobilities) because of the electron-rich nitrogen. In fact, a series of studies have been reported in the literature that involve such a donor–acceptor molecular architecture. For instance, Mori *et al.*[4] prepared copolymers with anthracene units embedded in the polymeric backbone along with side chains of triphenylamine, carbazole, or phenothiazine moieties. The resulting materials exhibited characteristic photoluminescence energy transfer, as confirmed by UV-vis and photoluminescence measurements. Tao *et al.*[5] and Lee *et al.*[6] synthesized a series of molecular dyads based on anthracene–triphenylamine derivatives and used these materials to make highly efficient blue organic light-emitting diodes. In other studies,[7,8] it was found that molecular dyads with anthracene derivatives and triarylamine hole stabilizers linked by π-conjugated bithiophene bridges exhibited superior intramolecular charge transfer from triarylamine to anthracene, which might be exploited for the preparation of small-molecule organic solar cells. Intramolecular electron and energy transfer was also observed with triphenylamine-bound zinc porphyrins.[9] For instance, Ezoe *et al.*[10] prepared a diarylurea-linked zinc porphyrin–anthracene dyad and observed intramolecular excitation energy transfer from anthracene to the zinc chromophore.

In these earlier studies, the efficiency of intramolecular energy/electron transfer and hence the optical/electronic properties of the molecular dyads are sensitively dependent upon the nature of the chemical bridges that link the donor and acceptor moieties. Although conventionally such chemical

[a] *Department of Chemistry and Biochemistry, University of California, 1156 High Street, Santa Cruz, California, USA. E-mail: bphebus@ucsc.edu, ysong4@ucsc.edu, phu@ucsc.edu, yabdolla@ucsc.edu, shaowei@ucsc.edu; Fax: +1 8314592935; Tel: +1 8314591892, +1 8314595841*

[b] *Department of Chemistry, Shantou University, Shantou, Guangdong, China. E-mail: 10yyuan1@stu.edu.cn, qxtong@stu.edu.cn*

† Electronic supplementary information (ESI) available: Representative TEM micrographs, X-ray diffraction (XRD) and small-angle X-ray scattering (SAXS) profiles, as well as NMR spectra. See DOI: 10.1039/c3cp52584h

linkers are aliphatic fragments that covalently bond to the donor and acceptor termini, nonbonding interactions have also been used as a tool to arrange donor–acceptor dyads, such as H-bonding, salt bridges, and hydrophobic interactions.[11–15] For instance, Kercher *et al.*[16] used a coordination compound, a scandium(III) acetylacetonate derivative, as the core and promoter of the dyad formation by noncovalent assembly of both an energy-donating ruthenium(II) bipyridine complex and an energy-accepting anthracene derivative, and observed effective quenching of the photoluminescence of the ruthenium chromophore by a fast intercomponent triplet–triplet energy-transfer process. In a more recent study,[17] a one-pot procedure was developed to prepare multifunctional surface-crosslinked micelles with 9,10-bis(4-methylphenyl)anthracene as the chromophores and Eosin Y disodium salt as the energy acceptor. The resulting nanostructures exhibited effective Förster energy transfer under photoirradiation and thus may be exploited as artificial light-harvesting systems.

With this arises an immediate question: is it possible to use metal nanoparticles as a unique structural scaffold to create functional dyads (or even polyads)? There are at least two advantages. First, similar to the above study where an organometallic complex is used as the core to form a dyad structure,[16] such a nanoscale architecture will significantly reduce the synthetic effort. Furthermore, it has long been known that nanoparticles can be chemically decorated with multiple functional groups,[18,19] which renders it possible to incorporate diverse and multiple functional moieties onto the nanoparticle surface, leading to the ready formation of a wide range of dyad (polyad) structures. More significantly, recently it has been found that organic functional ligands may be bound onto the metal core surface by different interfacial bonding interactions. Such unique chemistry may be exploited for further manipulation of the electronic interactions between the particle-bound functional moieties and hence the nanoparticle optical and electronic properties. Specifically, when functional groups are bound onto the nanoparticle surface by π conjugated metal–ligand bonds, effective intraparticle charge delocalization occurs between the particle-bound functional moieties.[20–23] For instance, when ferrocenyl moieties are attached onto ruthenium nanoparticle surfaces by conjugated metal–carbene or –vinylidene linkages, apparent intervalence charge transfer can be observed in electrochemical and near-infrared spectroscopic measurements.[20–23] Importantly, the behaviours are highly comparable to those observed in conventional intervalence systems based on organometallic complexes with conjugated chemical linkers, suggesting equally effective electronic coupling with nanosized metal cores as the chemical bridge *versus* conventional chemical bridges. In addition, such intraparticle charge delocalization can be further manipulated by the core valence states or external electrostatic polarization.[24–26] This is in sharp contrast to mercapto-functionalized nanoparticles in which the metal–sulfur bonds lack interesting chemistry.

It is within this context that this work was designed and carried out. In the present study, both derivatives of triphenylamine and anthracene were covalently bound onto ruthenium nanoparticle surfaces by conjugated metal–ligand bonds by olefin metathesis reactions of 1-decyne-functionalized ruthenium nanoparticles with 4-ethynyl-*N*,*N*-diphenylaniline and vinylanthracene. Spectroscopic as well as photoelectrochemical measurements indicated that upon photoirradiation, effective intraparticle charge transfer occurred from the triphenylamine group to the anthracene moiety, a behaviour consistent with those of conventional molecular dyads.

Experimental section

Chemicals

Ruthenium chloride hydrate ($RuCl_3 \cdot xH_2O$, ACROS), sodium acetate (NaOAc, 99.0%, MC&B), 9-vinylanthracene (VAN, 97%, Sigma-Aldrich), 1-decyne (95.0%, TCI America), 1,2-propanediol (99.5%, Sigma-Aldrich), triphenylamine (TPA, 98%, Sigma-Aldrich), and other solvents were obtained from typical commercial sources and used without further treatment. Water was supplied by a Barnstead Nanopure water system (18.3 MΩ cm). The synthesis and characterization of 4-ethynyl-*N*,*N*-diphenylaniline (EDPA) has been described previously in detail.[27]

Ruthenium nanoparticles

The synthetic procedure of ruthenium nanoparticles has been detailed previously.[22] In brief, a round bottom flask with 170 mL of 1,2-propanediol was set in a heating mantle with a slow bubbling of nitrogen. 0.05 g of $RuCl_3$ dissolved in a small amount of ethanol was then added into the flask, along with a six-molar equivalent of sodium acetate. The solution was subjected to thermal refluxing for 2 h, and the appearance of a dark brown colour signified the formation of ''bare'' ruthenium colloids. The solution was then cooled down to room temperature, and a calculated amount of 1-decyne (typically at threefold molar excess of $RuCl_3$) dispersed in 20 mL of toluene was added into the solution. The solution was then mixed by magnetic stirring overnight, resulting in the extraction of the nanoparticles into the toluene phase, as manifested by the dark brown colour in the toluene phase and the colourless appearance of the propanediol phase. This was due to the self-assembly of 1-decyne onto the ruthenium colloid surface forming ruthenium–vinylidene conjugated bonds at the metal–ligand interface.[22] The toluene phase was then collected and the solvents were removed by rotary evaporation. The resulting solids were then rinsed extensively with methanol to remove excess free ligands, affording 1-decyne-passivated ruthenium nanoparticles, which were denoted as RuHC10.

Surface functionalization of the RuHC10 nanoparticles was then carried out by metathesis reactions of the nanoparticles with olefin or acetylene derivatives (Scheme 1).[22] In a typical experiment, 20 mg of RuHC10 nanoparticles was dispersed in 3 mL of dichloromethane with a calculated amount of EDPA, VAN or a binary mixture of EDPA and VAN (at a molar ratio of 1 : 1) under magnetic stirring for 2 d. The resulting nanoparticles after purification were denoted as Ru(EDPA), Ru(VAN), and Ru(EDPA/VAN), respectively. The average core size of the nanoparticles was 1.90 ± 0.34 nm for Ru(EDPA), 2.01 ± 0.35 nm for Ru(VAN), and 1.97 ± 0.36 nm for Ru(EDPA/VAN) nanoparticles,

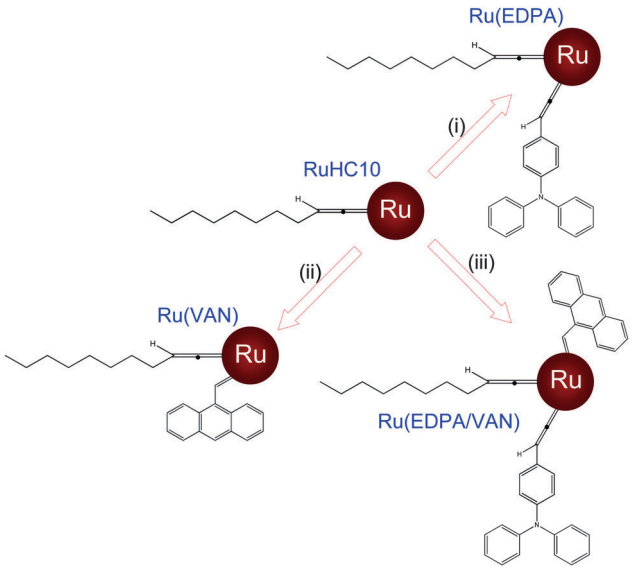

Scheme 1 Schematic of ruthenium nanoparticles functionalized with (i) EDPA, (ii) VAN or (iii) both.

as determined by transmission electron microscopic measurements (Fig. S1, ESI†).[22] Consistent results were observed in small-angle X-ray scattering (SAXS) measurements (Fig. S2, ESI†) where the average nanoparticle diameter was estimated to be 1.80 nm; and the metallic nature of the nanoparticle cores was confirmed using powder X-ray diffraction measurements (Fig. S3, ESI†).

Spectroscopy

^{1}H NMR measurements were performed with a Varian Unity 500 MHz NMR spectrometer using concentrated solutions of the nanoparticles in CD_2Cl_2. The absence of any sharp spectral features indicated that the nanoparticles were free from excess ligands.[22] To quantify the surface concentration of the functional ligands, the nanoparticle cores were dissolved in dilute aqueous KCN solution and the organic components were extracted by CH_2Cl_2 for ^{1}H NMR measurements (Fig. S4, ESI†). Based on the ratios of the integrated peak areas of the aromatic protons and the methyl protons, the surface coverage of the triphenylamine moieties of the Ru(EDPA) nanoparticles was estimated to be 41.0%; in Ru(VAN), the concentration of the anthracene moieties was about 9.9%; and in Ru(EDPA/VAN), the coverages of the triphenylamine and anthracene moieties were 25.2% and 35.8%, respectively.[20,28,29] UV-Vis spectra were acquired with an ATI Unicam UV4 spectrometer at 2 nm resolution by using a 1 cm quartz cuvette. Photoluminescence measurements were carried out using a PTI fluorospectrometer with the same solutions as those for UV-vis studies. FTIR spectra were obtained using a Perkin-Elmer Spectrum One FTIR spectrometer at a resolution of 1 cm^{-1}, where the samples were prepared by dropcasting a concentrated solution of the nanoparticles onto a ZnSe disk.

Electrochemistry

Electrochemical studies were carried out with a CHI 710 Electrochemical Workstation using a 3 mL quartz cuvette as the electrochemical cell. A gold disk sealed in glass tubing was used as the working electrode which was bent at the end so that the gold disk was facing sideways (for photoirradiation). The electrode was first polished by 0.03 μm alumina slurries and then sonicated in nanopure water. The gold electrode was further treated by rapid potential cycling in H_2SO_4 within the potential range of −0.2 V to +1.2 V at a potential sweep rate of 10 V s^{-1}, until a well-defined voltammetric feature for a clean gold surface was obtained, from which the effective electrochemical surface area was determined (*ca.* 1.3 mm^2). A Ag/AgCl wire and a platinum coil were used as the reference and counter electrode, respectively. The electrolyte solution was deaerated with nitrogen for 5 min and then blanketed with an atmosphere of nitrogen during the entire experimental procedure. The voltammograms were acquired both in the dark and under UV photoirradiation (365 nm, 6 W).

Results and discussion

Previously it has been found that acetylene derivatives may self-assemble on metal nanoparticle surfaces forming metal–vinylidene interfacial linkages by a tautomeric rearrangement process, and the resulting nanoparticles can undergo metathesis reactions with other acetylene or vinyl derivatives for further surface functionalization, with the functional units bound onto the nanoparticle surface by conjugated metal–carbon π bonds (Scheme 1).[22,30] As mentioned earlier, the successful incorporation of the triphenylamine and anthracene moieties onto the ruthenium nanoparticle surface was firstly confirmed using ^{1}H NMR measurements, where the surface coverages of the triphenylamine and anthracene moieties were 25.2% and 35.8%, respectively. The structures of the organic capping ligands were further examined using FTIR spectroscopy measurements. Fig. 1 depicts the FTIR spectra of the monofunctionalized Ru(EDPA) and Ru(VAN), and bifunctionalized Ru(EDPA/VAN) nanoparticles, along with those of monomeric EDPA and VAN. There are several

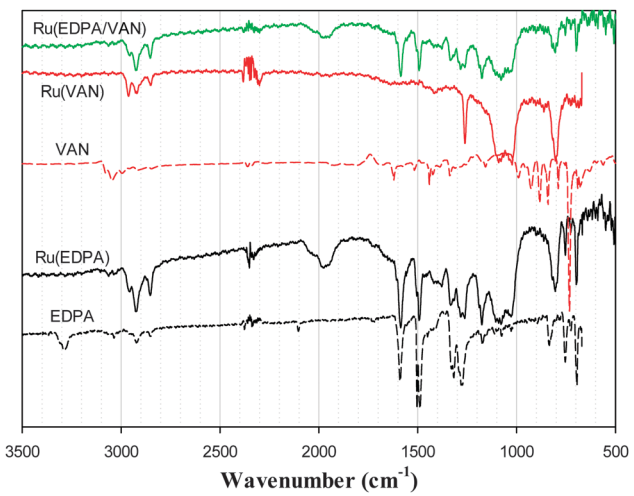

Fig. 1 FTIR spectra of Ru(EDPA), Ru(VAN) and Ru(EDPA/VAN) nanoparticles (solid curves), along with those of the monomeric EDPA and VAN ligands (dashed curves).

features that warrant special attention here. First, for the three nanoparticle samples (solid curves), three spectral features can be identified between 2100 cm^{-1} and 1900 cm^{-1} at 2056 cm^{-1}, 1976 cm^{-1} and 1950 cm^{-1}, which were accounted for by the self-assembly of the terminal acetylene moieties onto the Ru particle surface forming ruthenium–vinylidene (Ru═C═CH–, Scheme 1) interfacial linkages.[22,30] For comparison, the C≡C vibration of EDPA monomers (dashed black curve) can be found at 2104 cm^{-1} (and for 1-alkynes, this typically appears at *ca.* 2119 cm^{-1}). The apparent red-shift of the vibrational features of the nanoparticle-bound C≡C moieties as compared to those of monomers of acetylene derivatives was ascribed to the intraparticle charge delocalization as a result of the conjugated metal–ligand interfacial bonding interactions, as observed previously.[22,30]

Second, in contrast to the spectral profiles of monomeric EDPA and VAN ligands (dashed curves), a new vibrational band can be clearly seen at 804 cm^{-1} for the three nanoparticles (solid curves). This may be ascribed to the bending vibration of the vinylidene ═C–H moiety (Scheme 1), in good agreement with results of trisubstituted alkenes.[31] In fact, such a spectral feature has also been observed previously with ruthenium nanoparticles functionalized with 1-alkynes (though it was not explicitly identified at that time),[30] whereas for ruthenium nanoparticles functionalized with acetylide derivatives (*i.e.*, deprotonated alkynes),[21] no such feature was observed as no vinylidene moieties were formed at the metal–ligand interface.

Third, the nanoparticles exhibited no features around 3300 cm^{-1}, indicating that the samples were free from excess monomeric ligands (note that EDPA monomers display a band at 3288 cm^{-1} which is due to the terminal ≡C–H vibration).[30] In addition, the aromatic C═C vibrational stretches can be identified between 1400 cm^{-1} and 1600 cm^{-1} for both the nanoparticles and monomeric ligands, again, consistent with the incorporation of EDPA and VAN ligands onto the nanoparticle surface.

The optical properties of the chemically-functionalized nanoparticles were then investigated by UV-vis and photoluminescence spectroscopy measurements. Fig. 2 depicts the UV-vis absorption spectra of the Ru(EDPA), Ru(VAN) and Ru(EDPA/VAN) nanoparticles as well as the monomeric EDPA and VAN ligands. First, it can be seen that the three nanoparticle samples all exhibited an exponential-decay profile, due to the so-called Mie scattering as anticipated for nanosized metal nanoparticles.[32] Second, EDPA monomers (black dashed curve) exhibit a broad absorption band at *ca.* 322 nm, which is ascribed to the n–π* transition involving the central N atom.[5,33] In the Ru(EDPA) nanoparticles (solid black curve), this band blue-shifted somewhat to 302 nm, which is similar to results reported for triphenylamine oligomers bridged by conjugated linkers.[34] For monomeric VAN (dashed red curve), several absorption features can be identified between 350 nm and 400 nm which may be ascribed to the π–π* vibronic transitions of the molecules, and such characteristics can also be vaguely observed for the Ru(VAN) nanoparticles (solid red curve).[29] For the Ru(EDPA/VAN) nanoparticles (solid green curve), one can see that the absorption features of both the triphenylamine and anthracene cores can be identified in the regions of 300–330 nm and 330–400 nm, respectively. Again, this is consistent with the successful incorporation of both functional moieties onto the nanoparticle surface.

As both functional moieties were bound onto the ruthenium nanoparticle surface by Ru═C π bonds, effective intraparticle charge transfer likely occurred from the electron-donating triphenylamine unit to the electron-accepting anthracene moiety upon photoirradiation, as revealed in photoluminescence measurements. From Fig. 3, it can be seen that for the monofunctionalized nanoparticles of Ru(EDPA) and Ru(VAN), the photoluminescence profiles were characteristic of the respective functional moiety, though with some discrepancy. For instance, monomeric EDPA ligands showed a well-defined excitation peak (λ_{ex}) at 330 nm and a prominent emission one (λ_{em}) at 400 nm (dashed black curves), whereas for the Ru(EDPA) nanoparticles, the excitation peak position was found to be red-shifted somewhat to 340 nm, and the corresponding emission spectrum exhibited two major peaks at

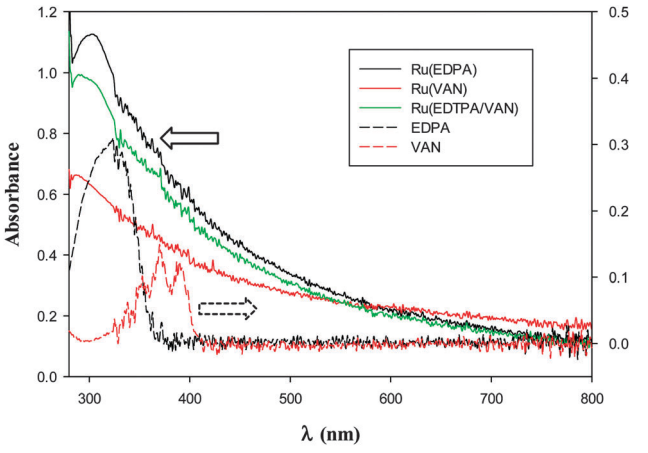

Fig. 2 UV-Vis absorption spectra of Ru(EDPA), Ru(VAN), and Ru(EDPA/VAN) nanoparticles (solid curves), as well as monomeric EDPA and VAN (dashed curves) in CH_2Cl_2. The left *y* axis is for the nanoparticles whereas the right *y* axis is for the monomeric ligands.

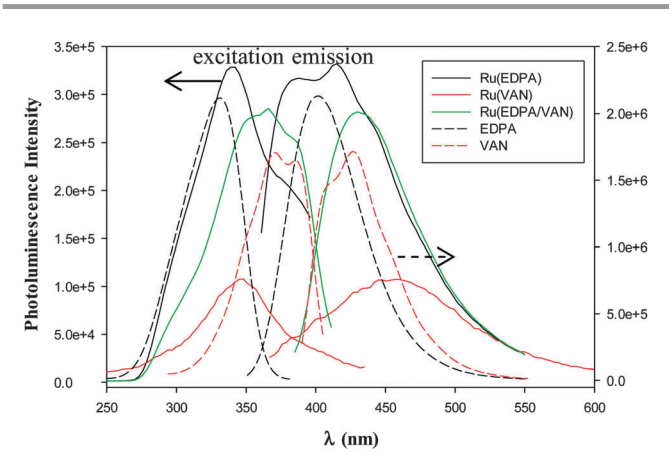

Fig. 3 Excitation and emission spectra of Ru(EDPA), Ru(VAN), and Ru(EDPA/VAN) nanoparticles (solid curves), as well as monomeric EDPA and VAN (dashed curves) in CH_2Cl_2. The left *y* axis is for the nanoparticles whereas the right *y* axis is for the monomeric ligands. The solutions were the same as those in Fig. 2.

Table 1 Summary of excitation and emission peak positions of Ru(EDPA), Ru(VAN), and Ru(EDPA/VAN) nanoparticles and the corresponding monomeric ligands

	EDPA	VAN	Ru(EDPA)	Ru(VAN)	Ru(EDPA/VAN)
λ_{ex} (nm)	330	371, 385	340	347	365
λ_{em} (nm)	400	409, 427	384, 414	460	431

384 nm and 414 nm, along with a shoulder at 442 nm (solid black curves), as summarized in Table 1. In contrast, for monomeric VAN (dashed red curves), two excitation peaks can be found at 371 and 385 nm and two emission peaks at 409 and 427 nm; however for the Ru(VAN) nanoparticles (solid red curves), the excitation peak position blue-shifted rather markedly to 347 nm and the emission profiles entailed a broad band centered at around 460 nm (Table 1). This is somewhat different from that observed in a previous study with carbene-stabilized ruthenium nanoparticles that were partially functionalized with vinylanthracene,[29] where a small red-shift was actually observed of the excitation peak position for the particle-bound anthracene moieties along with a decreasing Stokes shift between the emission and excitation peaks, as compared to those of the monomeric ligands. While the details are not clear at this point, this discrepancy may be due to the interactions between the π electrons of the anthracene and vinylidene/carbene moieties and hence different chemical environments for the anthracene units.

For the nanoparticles co-functionalized with both EDPA and VAN (green curves), the photoluminescence properties are more complicated, as depicted by the green curves. The most prominent excitation and emission peaks can be found at 365 nm and 431 nm (Table 1). Both the excitation and emission profiles resemble neither those of Ru(EDPA) nor those of Ru(VAN) in panel (A), suggesting a rather efficient mixing of the electronic energy levels of the particle-bound triphenylamine and anthracene moieties and hence the formation of new energy structures, most probably as a result of the conjugated metal–ligand (Ru═C) interfacial bonds. In fact, one can see that the excitation peak position was at a lower energy level than those of Ru(EDPA) and Ru(VAN), whereas the emission peak position was in the intermediate range between those of Ru(EDPA) and Ru(VAN). These observations suggest that the Ru(EDPA/VAN) nanoparticles behaved analogously to molecular dyads based on the triphenylamine–anthracene pairs with a conjugated chemical linker, and effective transfer of charge rather than energy occurred between the particle-bound triphenylamine and anthracene moieties.

For comparison, in a recent study Tang and co-workers[35] designed and synthesized star-shaped tris(4-anthracene-phenyl)-amine, a compound with a triphenylamine core decorated with three peripheral anthracene units. Because of a large dihedral angle between the triphenylamine and anthracene moieties, there was little electronic coupling between them. Thus only a single prominent photoluminescence emission peak was observed at 464 nm in chloroform, along with three absorption peaks at 350 nm, 368 nm, and 388 nm in UV-vis absorption measurements, which were consistent with those of the anthracene units (another peak at 310 nm was assigned to the absorption of the triphenylamine unit). In contrast, for tris(4-phenanthrene-phenyl)amine where the triphenylamine core was decorated with phenanthrene, because the twist angle between the phenanthrene plane and the phenyl ring was small, extensive conjugation occurred between the triphenylamine moiety and the substituted phenanthrene, leading to the appearance of only one absorption peak at 345 nm, along with a photoluminescence emission peak at 425 nm, which was attributed to the π–π* transition of the entire molecule.

The observed intraparticle charge delocalization is likely facilitated by through-bond interactions.[20] In fact, this hypothesis was further supported by a control experiment where monomeric triphenylamine was added to a solution of Ru(VAN) nanoparticles and there were virtually no interactions between the triphenylamine and anthracene moieties. Fig. 4 depicts the excitation and emission spectra of Ru(VAN) nanoparticles in the absence and presence of 1 nM monomeric triphenylamine. It can be seen that at λ_{ex} = 347 nm, the emission profiles of the Ru(VAN) nanoparticles remained virtually unchanged regardless of the addition of triphenylamine monomers; and when collected at λ_{em} = 360 nm, the excitation curves remained the same as well (black and green curves). In addition, when excited at λ_{ex} = 303 nm, the mixed solution of Ru(VAN) nanoparticles and triphenylamine monomers exhibited an emission spectrum that is consistent with that of triphenylamine monomers showing a single peak at λ_{em} = 359 nm. These observations indicate that in the mixed solution of Ru(VAN) nanoparticles and triphenylamine monomers, the two functional moieties were in essence independent of each other with minimal energy transfer and through-space charge transfer did not occur.

Note that in previous studies,[22,30] we have demonstrated that the particle-bound acetylene moieties behaved analogously to diacetylene derivatives and exhibited apparent photoluminescence as a result of intraparticle charge delocalization. However, such emissions were not resolved here as those from

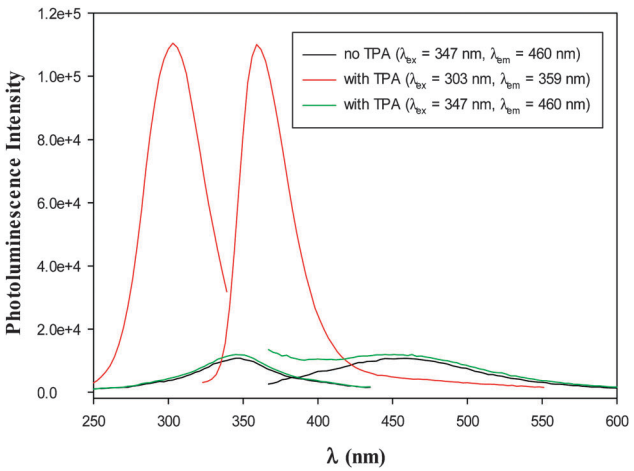

Fig. 4 Excitation and emission spectra of Ru(VAN) nanoparticles in the absence (black curves) and presence (red and green curves) of monomeric triphenylamine ligands in CH_2Cl_2. The concentration of the nanoparticle was 0.1 mg mL^{-1} and that of triphenylamine was 1 nM.

the triphenylamine and anthracene moieties were markedly more intense.

Electrochemical measurements further demonstrated that effective photo-induced intraparticle charge transfer occurred in Ru(EDPA/VAN) nanoparticles. Fig. 5 shows the cyclic voltammograms of a gold disk electrode in a deaerated solution of (A) monomeric EDPA, (B) Ru(EDPA) and (C) Ru(EDPA/VAN) in CH_2Cl_2 with 0.1 M TBAP in the dark (black curves) and upon the exposure to UV light irradiation (366 nm, red curves)—note that the triphenylamine moiety emits photoluminescence strongly under photoexcitation at this wavelength (Fig. 4). In panel (A), one can see that (i) a pair of voltammetric peaks appeared within the potential range of +0.70 and 1.50 V, (ii) the formal potential can be identified at +0.97 V in the dark and +1.02 V under UV photoirradiation, and (iii) the voltammetric peak currents remained virtually unchanged in the dark and under photoirradiation. These voltammetric features may be ascribed to the redox reaction of the triphenylamine moieties involving the formation of a cationic radical, $EDPA^{+\bullet} + e^- \leftrightarrow EDPA$.[33,35] The fact that the voltammetric profiles remained practically unchanged before and after photoirradiation indicated that the EDPA molecules were photochemically stable and the lifetime of the photoexcited state was significantly shorter than the voltammetric time scale.

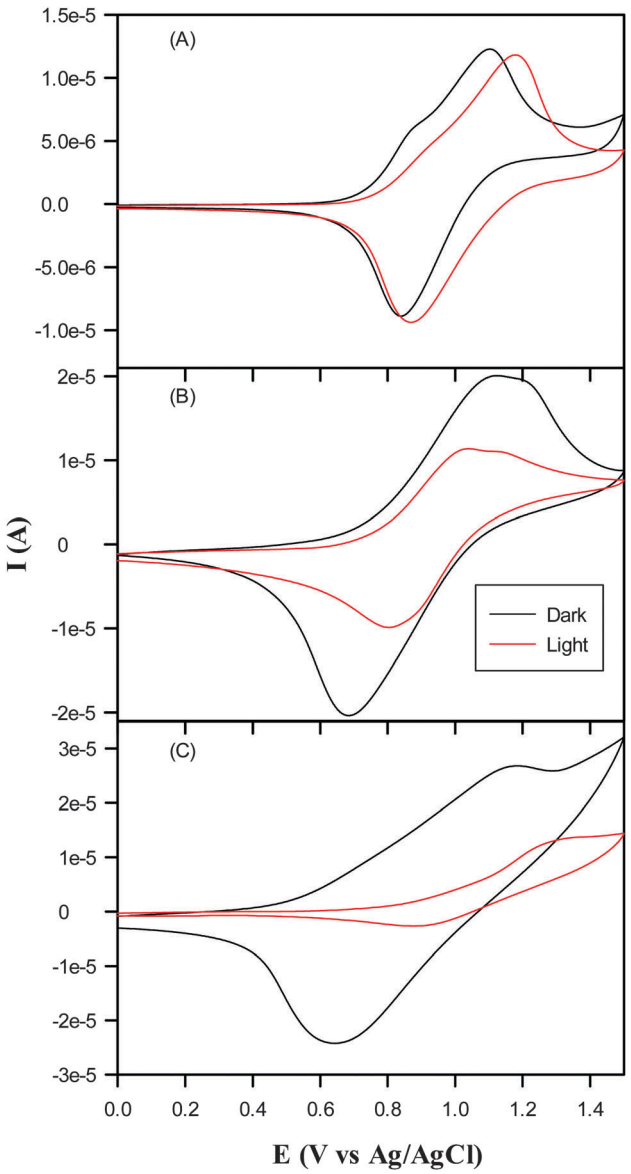

Fig. 5 Cyclic voltammograms acquired in the dark (black curves) and under photoirradiation (red curves) of (A) monomeric EDPA, (B) Ru(EDPA), and (C) Ru(EDPA/VAN) nanoparticles in CH_2Cl_2 with 0.1 M TBAP. The concentration of monomeric EDPA in (A) is *ca.* 2.2 mM, and the nanoparticle concentrations in (B) and (C) are both about 0.7 mg mL^{-1}. The area of the gold electrode was 1.3 mm^2, and potential sweep rate 50 mV s^{-1}.

In panel (B), Ru(EDPA) nanoparticles exhibited somewhat different voltammetric characteristics. Again, a pair of voltammetric peaks can be seen both in the dark and under UV photoirradiation, with the formal potentials very close to each other, at +0.90 and +0.92 V, respectively. Yet, the voltammetric currents diminished by about 50% under UV photoirradiation as compared to those acquired in the dark. Such behaviour is drastically different from that of monomeric EDPA in panel (A). First, the cathodic shift of 70–100 mV of the formal potentials, as compared to those of monomeric EDPA ligands, may be attributed to the conjugated metal–ligand interfacial bonding interactions that led to effective intraparticle charge delocalization. In addition, with conjugated interfacial bonding linkages, under UV photoirradiation, the photoexcited electrons might be effectively transferred from the triphenylamine units to the metal cores, leading to the apparent diminishments of the voltammetric currents. Note that it has been found previously that the metal core electrons serve as the effective conducting medium for intraparticle charge delocalization between particle-bound functional groups.[20]

With the attachment of electron-accepting anthracene moieties onto the nanoparticle surface also by conjugated metal–ligand interfacial bonds, the photoelectrochemical behaviours of the particle-bound triphenylamine moieties become more interesting. In panel (C), one can see that in the dark, again, a pair of voltammetric peaks can be identified with the formal potential of +0.91 V (which was close to that of Ru(EDPA) nanoparticles in panel (B)). However, under UV photoirradiation, the voltammetric peaks disappeared almost completely. This may be accounted for by the presence of electron-accepting anthracene moieties on the nanoparticle surface that further facilitate charge transfer from the photo-excited triphenylamine moieties to the nanoparticle cores and then to the anthracene centers. The photo-induced depletion of the triphenylamine valence electrons thus led to the almost complete diminishment of the corresponding voltammetric features. These results are consistent with the photoluminescence observations presented above, suggesting that with the nanoparticle cores serving as the conducting media, the particle-bound triphenylamine and anthracene moieties indeed behaved analogously to molecular dyads based on these two functional units bridged by conjugated chemical spacers. Overall, the structural architecture is analogous to that reported by Kercher *et al.*[16] where they used an organometallic coordination compound as

the core and promoter of the dyad formation by noncovalent assembly of both energy-donating and -accepting units.

Conclusions

When functional moieties are bound onto metal nanoparticle surfaces by conjugated metal–ligand interfacial bonding interactions, effective intraparticle charge delocalization occurs. For nanoparticles co-functionalized with derivatives of triphenylamine and anthracene, the resulting nanoparticles exhibited spectroscopic and electrochemical characteristics that are consistent with conventional molecular dyads based on the same electron-donating and -accepting units. Significantly, it was found that photoluminescence emission of the Ru(EDPA/VAN) nanoparticles was completely different from those of the monofunctionalized Ru(EDPA) and Ru(VAN) nanoparticles, suggesting effective mixing of the π electrons between the triphenylamine and anthracene moieties. Furthermore, in photoelectrochemical studies, the particle-bound triphenylamine moieties exhibited a pair of well-defined voltammetric peaks in the dark due to the redox reactions involving the formation of cationic radicals; however upon exposure to UV photoirradiation, the peak currents diminished drastically, which was ascribed to the rapid transfer of photogenerated electrons from the triphenylamine units to the anthracene ones. This is most likely facilitated by the conjugated metal–ligand bonds and hence low interfacial contact resistance. As the nanoparticles are known to serve as effective structural scaffolds for complicated chemical functionalization, the strategy presented in this study may be exploited for the development of multi-functional nanoparticle-based electronic systems that are challenging to produce using conventional organic complexes.[5–8] Such research is being pursued and the results will be reported in due course.

Acknowledgements

This work was supported, in part, by the National Science Foundation (CHE – 1265635, CHE – 1012258, and DMR – 0804049, S.W.C.), the National Natural Science Foundation of China (No. 91027041, Q.X.T.), and the ACS Petroleum Research Fund (49137 – ND10, S.W.C.).

References

1 F. M. Raymo and M. Tomasulo, *Chem. Soc. Rev.*, 2005, **34**, 327–336.
2 J. W. Verhoeven, *J. Photochem. Photobiol., C*, 2006, **7**, 40–60.
3 Y. Z. Lin, Y. F. Li and X. W. Zhan, *Chem. Soc. Rev.*, 2012, **41**, 4245–4272.
4 H. Mori, I. Tando and H. Tanaka, *Macromolecules*, 2010, **43**, 7011–7020.
5 S. Tao, Y. C. Zhou, C. S. Lee, S. T. Lee, D. Huang and X. H. Zhang, *J. Phys. Chem. C*, 2008, **112**, 14603–14606.
6 K. H. Lee, J. N. You, H. J. Kwon, Y. K. Kim and S. S. Yoon, *Mol. Cryst. Liq. Cryst.*, 2010, **530**, 204–211.
7 H. Choi, H. M. Ko, N. Cho, K. Song, J. K. Lee and J. Ko, *ChemSusChem*, 2012, **5**, 2045–2052.
8 K. R. J. Thomas, P. Singh, A. Baheti, Y. C. Hsu, K. C. Ho and J. T. Lin, *Dyes Pigm.*, 2011, **91**, 33–43.
9 C. W. Huang, K. Y. Chiu and S. H. Cheng, *Dalton Trans.*, 2005, 2417–2422.
10 M. Ezoe, T. Minami, Y. Ogawa, S. Yagi, H. Nakazumi, T. Matsuyama, K. Wada and H. Horinaka, *Photochem. Photobiol. Sci.*, 2005, **4**, 641–646.
11 T. H. Ghaddar, E. W. Castner and S. S. Isied, *J. Am. Chem. Soc.*, 2000, **122**, 1233–1234.
12 M. D. Ward and F. Barigelletti, *Coord. Chem. Rev.*, 2001, **216**, 127–154.
13 H. F. M. Nelissen, A. F. J. Schut, F. Venema, M. C. Feiters and R. J. M. Nolte, *Chem. Commun.*, 2000, 577–578.
14 A. E. Kaifer, *Acc. Chem. Res.*, 1999, **32**, 62–71.
15 R. Billing, D. Rehorek and H. Hennig, *Top. Curr. Chem.*, 1990, **158**, 151–199.
16 M. Kercher, B. Konig, H. Zieg and L. De Cola, *J. Am. Chem. Soc.*, 2002, **124**, 11541–11551.
17 H. Q. Peng, Y. Z. Chen, Y. Zhao, Q. Z. Yang, L. Z. Wu, C. H. Tung, L. P. Zhang and Q. X. Tong, *Angew. Chem., Int. Ed.*, 2012, **51**, 2088–2092.
18 A. C. Templeton, M. P. Wuelfing and R. W. Murray, *Acc. Chem. Res.*, 2000, **33**, 27–36.
19 V. M. Rotello, *Nanoparticles: building blocks for nanotechnology*, Kluwer Academic/Plenum Publishers, New York, 2004.
20 W. Chen, S. W. Chen, F. Z. Ding, H. B. Wang, L. E. Brown and J. P. Konopelski, *J. Am. Chem. Soc.*, 2008, **130**, 12156–12162.
21 W. Chen, N. B. Zuckerman, X. W. Kang, D. Ghosh, J. P. Konopelski and S. W. Chen, *J. Phys. Chem. C*, 2010, **114**, 18146–18152.
22 X. W. Kang, N. B. Zuckerman, J. P. Konopelski and S. W. Chen, *J. Am. Chem. Soc.*, 2012, **134**, 1412–1415.
23 X. W. Kang, Y. Song and S. W. Chen, *J. Mater. Chem.*, 2012, **22**, 19250–19257.
24 X. W. Kang, N. B. Zuckerman, J. P. Konopelski and S. W. Chen, *Angew. Chem., Int. Ed.*, 2010, **49**, 9496–9499.
25 X. W. Kang, W. Chen, N. B. Zuckerman, J. P. Konopelski and S. W. Chen, *Langmuir*, 2011, **27**, 12636–12641.
26 X. W. Kang, X. Li, W. M. Hewitt, N. B. Zuckerman, J. P. Konopelski and S. W. Chen, *Anal. Chem.*, 2012, **84**, 2025–2030.
27 Q. X. Tong, M. Y. Chan, S. L. Lai, T. W. Ng, P. F. Wang, C. S. Lee and S. T. Lee, *Dyes Pigm.*, 2010, **86**, 233–237.
28 W. Chen, N. B. Zuckerman, J. W. Lewis, J. P. Konopelski and S. W. Chen, *J. Phys. Chem. C*, 2009, **113**, 16988–16995.
29 W. Chen, S. Pradhan and S. W. Chen, *Nanoscale*, 2011, **3**, 2294–2300.
30 X. W. Kang and S. W. Chen, *Nanoscale*, 2012, **4**, 4183–4189.
31 P. Larkin, *Infrared and raman spectroscopy: principles and spectral interpretation*, Elsevier, Amsterdam, Boston, 2011.
32 J. A. Creighton and D. G. Eadon, *J. Chem. Soc., Faraday Trans.*, 1991, **87**, 3881–3891.
33 W. Z. Gao, S. R. Wang, Y. Xiao and X. G. Li, *Spectrochim. Acta, Part A*, 2012, **98**, 215–221.
34 W. Z. Gao, X. G. Li, S. R. Wang and H. J. Lv, *Chin. Chem. Lett.*, 2012, **23**, 141–144.
35 S. Tang, W. J. Li, F. Z. Shen, D. D. Liu, B. Yang and Y. G. Ma, *J. Mater. Chem.*, 2012, **22**, 4401–4408.